

Adversarial Example Soups: Improving Transferability and Stealthiness for Free

Bo Yang*, Hengwei Zhang*, Jindong Wang, Yulong Yang, Chenhao Lin, *Member, IEEE*, Chao Shen, *Senior Member, IEEE*, Zhengyu Zhao, *Member, IEEE*

Abstract—Transferable adversarial examples cause practical security risks since they can mislead a target model without knowing its internal knowledge. A conventional recipe for maximizing transferability is to keep only the optimal adversarial example from all those obtained in the optimization pipeline. In this paper, for the first time, we question this convention and demonstrate that those discarded, sub-optimal adversarial examples can be reused to boost transferability. Specifically, we propose “Adversarial Example Soups” (AES), with AES-tune for averaging discarded adversarial examples in hyperparameter tuning and AES-rand for stability testing. In addition, our AES is inspired by “model soups”, which averages weights of multiple fine-tuned models for improved accuracy without increasing inference time. Extensive experiments validate the global effectiveness of our AES, boosting 10 state-of-the-art transfer attacks and their combinations by up to 13% against 10 diverse (defensive) target models. We also show the possibility of generalizing AES to other types, *e.g.*, directly averaging multiple in-the-wild adversarial examples that yield comparable success. A promising byproduct of AES is the improved stealthiness of adversarial examples since the perturbation variances are naturally reduced.

Index Terms—Adversarial example soups, black-box attacks, transferability, stealthiness.

I. INTRODUCTION

In recent years, Deep Neural Networks (DNNs) have achieved considerable success in various computer vision tasks, such as image classification [1], [2], face recognition [3], [4], and object detection [5], [6]. However, DNNs are known to be vulnerable to adversarial examples [7]–[11], which are crafted by adding imperceptible perturbations into clean images. Adversarial examples can cause severe threats in practice due to their transferability, *i.e.*, the adversarial examples generated on the surrogate model can be directly used to mislead unknown target models [12]–[16].

Transferable adversarial examples have been extensively studied [18]–[24], with new attack methods continuously proposed based on diverse ideas, such as gradient stabilization [25], [26], input transformation [27], [28], and feature disruption [29], [30]. In general, generating a (transferable) adversarial example is a gradient-based optimization problem.

Bo Yang, Hengwei Zhang, and Jindong Wang are with the State Key Laboratory of Mathematical Engineering and Advanced Computing, Zhengzhou, China.

Yulong Yang, Chenhao Lin, Chao Shen, and Zhengyu Zhao are with the School of Cyber Science and Engineering, Xi’an Jiaotong University, Xi’an, China.

*The first two authors contribute equally.

Corresponding authors: Hengwei Zhang (wlby_zzmy_henan@163.com) and Zhengyu Zhao (zhengyu.zhao@xjtu.edu.cn)

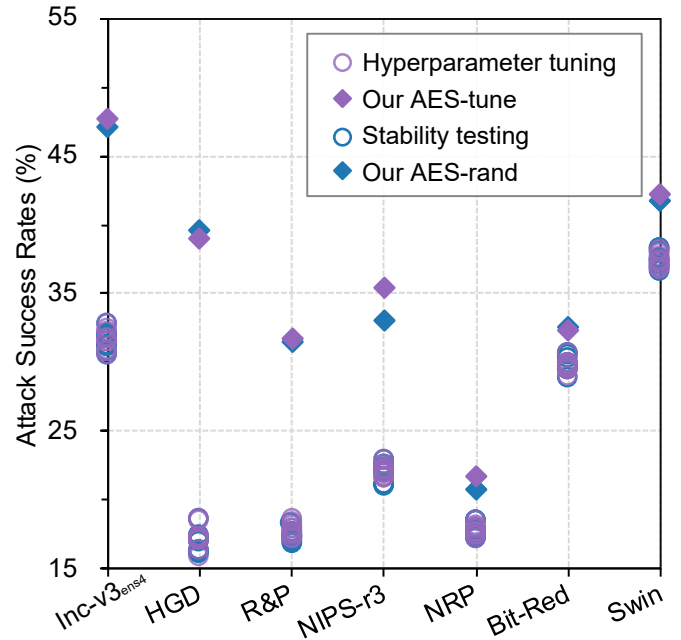


Fig. 1. Our Adversarial Example Soups (AES) attack consistently improves the transferability from Inc-v3 to diverse (defensive) target models on ImageNet. AES-tune (AES-rand) averages 10 sessions of adversarial examples from hyperparameter tuning (stability testing). Here we report the results for the well-known DIM [17] attack and other attacks also yield similar patterns.

Therefore, when a new transferable attack is proposed, existing work follows the conventional optimization recipe to conduct hyperparameter tuning and stability testing. Specifically, hyperparameter tuning is conducted to select the hyperparameter(s) that ensure optimal transferability, and stability testing is conducted to study the sensitivity of the proposed attack to potential randomness in the whole attack pipeline. We examine 30 representative transfer studies and notice that hyperparameter tuning is conducted in all of them, and stability testing is also often conducted, *e.g.*, in [31]–[33].

Such a conventional optimization recipe normally consumes substantial resources of computation and time. However, existing attacks keep only the final optimal adversarial example but discard all the rest contained through the process. In this paper, for the first time, we question this conventional recipe and demonstrate that it is possible to “*turn trash into treasure*”, *i.e.*, leveraging those discarded, sub-optimal adversarial examples to boost transferability for free.

To this end, we propose “Adversarial Example Soups” (AES), which reuse multiple discarded adversarial examples

by simply averaging them, including the optimal one. Specifically, AES-tune reuses the discarded samples in hyperparameter tuning, and AES-rand targets stability testing. As shown in Figure 1, both AES-tune and AES-rand improve their corresponding baselines, i.e., hyperparameter tuning and stability testing, by a large margin. For the averaging operation, we explore three common strategies, i.e., uniform, weighted, and greedy. Extensive experiments involving 10 state-of-the-art transferable attacks and 10 diverse (defensive) target models validate the global effectiveness of our AES. We also investigate a practically promising scenario where multiple in-the-wild adversarial examples with a similar level of success from arbitrary attacks can also be averaged to boost their transferability. In addition to improving attack transferability, AES improves attack stealthiness because the perturbation variances are naturally reduced through the averaging operation.

AES is inspired by “model soups” [34], which can improve the accuracy and robustness of a model by simply averaging the weights of multiple models fine-tuned with different hyperparameter configurations. This idea can work in the context of transferability for the following reasons. Overall, it is well known that transferring an adversarial example from a known (surrogate) model to an unknown (target) model is conceptually similar to generalizing a model from known (training) examples to unknown (testing) examples [17], [25]. In this case, optimizing adversarial perturbations is analogous to optimizing model weights. In particular, the underlying assumption of “model soups” is that the weights of multiple fine-tuned models often lie in a single error basin [34]–[36], which also holds in our context of adversarial attacks (see experimental evidence in Section III-B).

In sum, we make the following main contributions:

- We, for the first time, question the conventional recipe for optimizing adversarial transferability, which only picks the optimal adversarial example but discards the rest (sub-optimal) ones during hyperparameter tuning and stability testing. Instead, we “*turn trash into treasure*”, i.e., leveraging those discarded adversarial examples to boost transferability for free.
- We propose “Adversarial Example Soups” (AES), a new approach to reusing multiple discarded adversarial examples by averaging them and the optimal one. We demonstrate the global effectiveness of AES in improving 10 state-of-the-art transferable attacks and their combinations on 10 diverse (defensive) target models.
- We further demonstrate the effectiveness of AES in improving attack stealthiness, and we discuss other potential types of AES, e.g., improving transferability by averaging multiple in-the-wild adversarial examples with comparable success rates generated by arbitrary attacks.

II. RELATED WORK

A. Adversarial Attacks

In general, adversarial attacks can be divided into white-box attacks and black-box attacks. Under the white-box setting, the adversary is familiar with all the information such as the

structure, parameters, and training data of the neural networks, which is difficult to achieve in the practical scenario. To overcome this limitation, black-box attacks have been explored and roughly divided into query-based attacks and transfer-based attacks. Compared with query-based attacks, transfer-based attacks have better stealthiness as they do not require querying the network, thus attracting significant attention from researchers [37]–[42]. However, further research is needed to investigate how to enhance adversarial transferability for effective black-box attacks.

Gradient stability attacks. Dong *et al.* [25] first introduce momentum into the iterative version of the Fast Gradient Sign Method (FGSM) to stabilize the gradient direction and generate more transferable adversarial examples. Lin *et al.* [26] adopt Nesterov accelerated gradient to further boost adversarial transferability. Wang *et al.* [43] employ variance tuning to find more stable gradient update directions, significantly increasing the success rates of adversarial attacks. Ge *et al.* [31] propose the Penalizing Gradient Norm (PGN) attack, which achieves a significant improvement in transferability.

Input transformation attacks. From the perspective of the similarity between adversarial transferability and model generalization, data augmentation techniques commonly used in neural network training are widely employed to enhance adversarial transferability. DIM [17] utilizes diversified inputs in adversarial attacks to alleviate overfitting to surrogate models. Lin *et al.* [26] optimize adversarial perturbations by using multiple scaled copies of inputs. Admix [44] mixes a group of randomly sampled images from other classes. Spectral Simulation Attack (SSA) [45] adjusts the image in the frequency domain to simulate more diverse substitute models.

Feature disruption attacks. Other methods enhance the transferability of adversarial examples from the perspective of feature disruption, known as feature disruption attacks. Specifically, FDA [46] indiscriminately manipulates the activations from internal layers to disrupt semantic image features. FIA [29] minimizes weighted feature mapping in intermediate layers to disrupt important object-aware features that dominate model classification. NAA [30] conducts feature-level attacks through a more accurate estimation of neuron importance. In this study, we demonstrate that our AES can boost the transferability and stealthiness of all the above three categories of attacks.

B. Adversarial Defenses

To mitigate the threat of adversarial attacks, numerous defense methods have been proposed. Among them, adversarial training (AT) methods [8], [11], [47], which iteratively incorporate adversarial examples into the training data, are widely used. Although AT is effective even against white-box attacks, it suffers from high training costs. Existing research has commonly agreed that AT is not necessary against black-box attacks. Therefore, more efficient defenses have been explored against black-box attacks. Specifically, Tramèr *et al.* [48] adopt AT but only generate one-time (transferable) adversarial examples for training. Other defenses rely on input preprocessing. Specifically, Liao *et al.* [49] utilize the High-Level Representation Guided Denoiser (HGD) to eliminate

TABLE I

THE ATTACK SUCCESS RATES/LOSS VALUES ACROSS MULTIPLE ADVERSARIAL EXAMPLES OBTAINED IN HYPERPARAMETER TUNING OF μ IN MI [25] AND STABILITY TESTING. INC-V3 IS THE SURROGATE MODEL.

	Inc-v3 _{adv}	Inc-v3 _{ens3}	Inc-v3 _{ens4}	IncRes-v2 _{ens}
$\mu = 0.91$	27.7/1.08	22.7/0.97	21.8/0.95	10.9/0.49
$\mu = 0.92$	26.5/1.08	23.0/0.94	22.1/0.96	10.7/0.48
$\mu = 0.93$	28.1/1.09	22.3/0.95	21.8/0.92	11.0/0.47
$\mu = 0.94$	27.1/1.09	22.4/0.92	21.8/0.94	11.4/0.46
$\mu = 0.95$	27.0/1.10	21.4/0.94	21.6/0.93	10.3/0.47
$\mu = 0.96$	27.2/1.10	23.0/0.93	22.1/0.95	11.0/0.49
$\mu = 0.97$	26.3/1.09	22.8/0.90	21.2/0.94	10.8/0.47
$\mu = 0.98$	26.6/1.11	23.8/0.92	21.5/0.93	10.8/0.49
$\mu = 0.99$	27.7/1.10	23.4/0.93	22.4/0.94	10.6/0.47
$\mu = 1.00$	27.3/1.12	22.7/0.94	23.0/0.95	11.4/0.47
Stability testing ($\mu = 1.00$)	26.7/1.13	22.5/0.92	22.3/0.96	11.2/0.47
	25.8/1.11	23.0/0.92	22.3/0.94	11.2/0.47
	27.9/1.12	23.2/0.94	22.8/0.93	11.2/0.48
	27.1/1.12	23.6/0.93	22.0/0.94	11.6/0.46
	27.1/1.10	22.1/0.95	22.4/0.93	11.1/0.47
	26.5/1.12	22.5/0.91	21.9/0.96	11.4/0.48
	27.2/1.12	22.2/0.91	22.4/0.94	11.2/0.47
	27.2/1.11	22.4/0.92	21.8/0.93	11.7/0.47
	27.1/1.11	21.6/0.95	21.5/0.95	11.3/0.48
	27.9/1.12	22.9/0.94	22.2/0.91	10.8/0.46

adversarial perturbations from input images. Xie *et al.* [50] employ random Resizing and Padding (R&P) on adversarial examples to reduce their effectiveness. Cohen *et al.* [51] present the Randomized Smoothing (RS) method to obtain ImageNet classifiers with certified adversarial robustness. Moreover, Naseer *et al.* [52] leverage a Neural Representation Purifier (NRP) model to purify adversarial examples. Xu *et al.* [53] design Bit-Reduction (Bit-Red) and Spatial Smoothing as defenses against adversarial examples. In this study, we evaluate our AES against diverse target models with the above state-of-the-art defenses.

III. ADVERSARIAL EXAMPLE SOUPS (AES)

A. Preliminary

Let x and y be the benign input and its corresponding true label, respectively, while θ represents the parameters of the classifier f . $L(\theta, x, y)$ denotes the loss function of the classifier f , typically the cross-entropy loss function. The objective of the adversary is to find an adversarial example x^{adv} that visually resembles but can mislead the model $f(x^{adv}; \theta) \neq y$ by maximizing $L(\theta, x, y)$. To maintain consistency with previous work [25], [26], we impose a constraint on the adversarial perturbation using the infinity norm, such that $\|x^{adv} - x\|_{\infty} \leq \epsilon$. Therefore, the generation of adversarial examples can be transformed into the following constrained maximization problem:

$$\arg \max_{x^{adv}} L(\theta, x^{adv}, y), \quad \text{s.t. } \|x^{adv} - x\|_{\infty} \leq \epsilon. \quad (1)$$

Directly solving the optimization problem of Eq. 1 is quite complex. Therefore, Goodfellow *et al.* [8], inspired by the training process of neural networks, propose the Fast Gradient Sign Method. This method increases the value of the loss function in the direction of gradient ascent to craft adversarial examples. Alexey *et al.* [54] extend the FGSM to an iterative version called I-FGSM, with the following update formula:

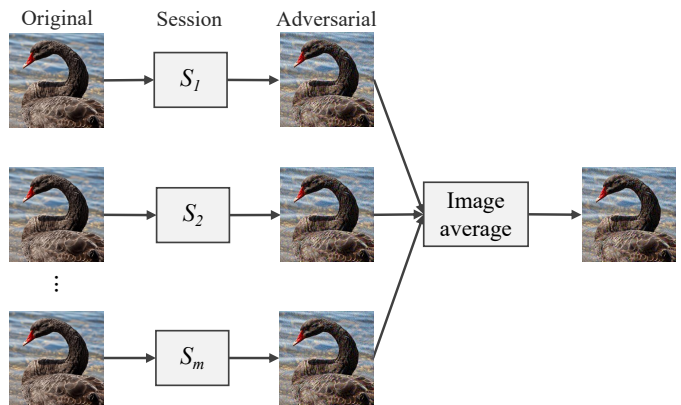


Fig. 2. The framework of our Adversarial Example Soups (AES) attack. AES averages m sessions of adversarial examples from a common optimization process, e.g., hyperparameter tuning or stability testing.

$$x_0^{adv} = x, x_{t+1}^{adv} = x_t^{adv} + \alpha \cdot \text{sign}(\nabla_x L(\theta, x_t^{adv}, y)), \quad (2)$$

where $\alpha = \epsilon/T$, in which T is the number of iterations. FGSM and I-FGSM are simple to use and have good scalability, which are the basis of subsequent iterative attack methods. Based on Eq. 2, the gradient stabilization attack is to optimize the gradient $\nabla_x L(\theta, x_t^{adv}, y)$ in Eq. 2. The input transformation attack is to transform the input x_t^{adv} at each iteration, and then compute the gradient of the transformed image. Feature destruction attacks use the features that the model focuses on to find a better gradient. Unlike existing transferable attacks, our approach focuses on the final output x_T^{adv} .

B. Motivation of AES

The key assumption of our AES is that the multiple adversarial examples obtained in the optimization pipeline should reside in the same error basin [34]–[36]. Here we conduct exploratory experiments to show this assumption is satisfied in both hyperparameter tuning and stability testing, which are commonly conducted in existing work on transferable attacks. Since the high dimensionality of images makes it difficult to visualize the loss landscape over pixels, we directly compare the model output, *i.e.*, the attack success rates and loss values. As shown in Table I, both the attack success rates and loss values are very close across different adversarial examples, suggesting that these adversarial examples are very likely to reside in the same error basin. This finding is also consistent with that for “model soups”, where multiple fine-tuned models initialized from the same pre-training often lie in the same error basin [35].

C. Technical Details of AES

As illustrated in Figure 2, Adversarial Example Soups (AES) averages the adversarial examples from multiple sessions that correspond to different configurations of hyperparameters in hyperparameter tuning or repeated experiments in stability testing. For the averaging strategy, we explore uniform, weighted, and greedy methods. Specifically, the uniform method averages pixel values at corresponding positions

of multiple adversarial images. The weighted and greedy methods further assign different weights to different sessions of adversarial examples based on their transferability ranking on a hold-out target model. Adversarial examples by and find the greedy method yields a slightly better performance since it leverages more knowledge. Note that all three averaging strategies can effectively boost the transferability of baseline attacks, the uniform averaging way is adopted in the main experiments since it is the most simple and convenient (see more details in Section IV-D).

AES-tune for hyperparameter tuning. In order to select the hyperparameter for optimal attack transferability of a new attack method, it is common to conduct hyperparameter tuning. Specifically, in each session of hyperparameter tuning, a specific hyperparameter value is selected from a pre-defined range and used to generate an adversarial example. Note that a hold-out target model is used for testing the transferability. In this case, AES-tune averages adversarial examples from multiple sessions of hyperparameter tuning.

AES-rand for stability testing. In order to make sure the transferability of a new attack is not sensitive to potential randomness in optimizing adversarial examples, stability testing is often conducted and results with variances are reported. Such randomness generally comes from the non-deterministic GPU calculations and the change between dependent libraries, such as PyTorch and NumPy. It can also come from the randomness of specific hyperparameters of an attack. For example, DI implements stochastic transformation with probability p at each iteration. In this case, AES-rand averages adversarial examples from multiple sessions of stability testing.

In addition to the above AES-tune and AES-rand, there may be other forms of AES. For example, the code for implementing different attack methods is publicly available, and adversarial images may be visualized anywhere. In this case, we show that it is possible to average such in-the-wild adversarial examples that already yield comparable success to further boost their transferability (see detailed discussion in Section V-B).

IV. EXPERIMENTS

In this section, we conduct extensive experiments to validate the effectiveness of our AES. Specifically, we validate the global effectiveness of AES in improving the transferability of gradient stabilization, input transformation, and feature disruption attacks (Section IV-B). In addition, we demonstrate the effectiveness of AES in improving the stealthiness of different attacks in Section IV-C. Finally, we conduct ablation studies to investigate the impact of important components and hyperparameters on the performance (Section IV-D). In the following, we first describe the experimental setups.

A. Experimental Setups

Dataset and models. Following the common practice [25], [43], [55], we randomly select 1000 images from the ImageNet validation set [56] that are correctly classified. For the surrogate model, we adopt four normally trained networks: Inception-v3 (Inc-v3) [57], Inception-v4 (Inc-v4) [58],

TABLE II
THE 10 HYPERPARAMETER CONFIGURATIONS IN AES-TUNE FOR DIFFERENT ATTACKS.

Attack	Hyperparameter configurations
MI [25]	Decay factor $\mu = 0.91, 0.92, \dots, 1.00$
NI [26]	Decay factor $\mu = 0.91, 0.92, \dots, 1.00$
VMI [43]	Number of sampled examples $N = 16, 17, \dots, 25$
PGN [31]	Balanced coefficient $\delta = 0.491, 0.492, \dots, 0.500$
DIM [17]	Resize rate $r = 1.132, 1.134, \dots, 1.150$
SIM [26]	Decay factor $\mu = 0.91, 0.92, \dots, 1.00$
Admix [44]	Mixing factor $\eta = 0.191, 0.192, \dots, 0.200$
SSA [45]	Tuning factor $\rho = 0.500, 0.505, \dots, 0.545$
FIA [29]	Drop probability $p_d = 0.255, 0.260, \dots, 0.300$
NAA [30]	Weighted attribution factor $\gamma = 0.91, 0.92, \dots, 1.00$

Inception-Resnet-v2 (IncRes-v2) [58], and Resnet-v2-152 (Res-152) [2]. For the target model, we consider challenging scenarios with defenses and different model architectures. Specifically, we consider adversarially trained models [48], *i.e.*, adv-Inception-v3 (Inc-v3_{adv}), ens3-adv-Inception-v3 (Inc-v3_{ens3}), ens4-adv-Inception-v3 (Inc-v3_{ens4}), and ens-adv-Inception-ResNet-v2 (IncRes-v2_{ens}), well-known defenses, *i.e.*, HGD [49], R&P [50], NIPS-r3¹, NRP [52], and Bit-Red [53], as a Swin Transformer (Swin) [59].

Baseline attacks. To demonstrate the global effectiveness of our AES, we select a variety of representative transferable attacks as our baselines. Specifically, for gradient stabilization attacks, we choose MI [25], NI [26], VMI [43], and PGN [31]. For input transformation attacks, we choose DIM [17], SIM [26], Admix [44], and SSA [45]. For feature disruption attacks, we choose FIA [29] and NAA [30].

Attack settings. We follow the common practice [17], [26], [31] to set the maximum magnitude of perturbation $\epsilon = 16$, the number of iterations $T = 10$, and the step size $\alpha = 1.6$. We adopt the default hyperparameter settings for different baseline attacks. Specifically, for MI and NI, we set the decay factor $\mu = 1.0$. For VMI, we set the hyperparameter $\beta = 1.5$ and the number of copies $N = 20$. For PGN, we set the number of copies $N = 20$, the balancing factor $\delta = 0.5$ and the upper bound of neighborhood size $\zeta = 3.0 \times \epsilon$. For DIM, we set the transformation probability $p = 0.5$. For SIM, we set the number of copies $N = 5$. For Admix, we set the mix ratio $\eta = 0.2$. For SSA, we set the tuning factor $\rho = 0.5$ and the number of spectrum transformations $N = 20$. For FIA, we set the drop probability $p_d = 0.3$ and the ensemble number $N = 30$. For NAA, we set the weighted attribution factor $\gamma = 1.0$ and the integrated steps $I = 30$. For our AES, we set the number of sessions $m = 10$, and the detailed hyperparameters for different attacks that form AES-tune are listed in Table II. Note that for other types of AES, the default settings of the baseline attacks are used.

B. AES Improves Transferability

Here we evaluate the effectiveness of our AES in improving the transferability of three categories of attacks: gradient

¹<https://github.com/anlthms/nips-2017/tree/master/mmd>

TABLE III
THE SUCCESS RATES (%) OF GRADIENT STABILIZATION ATTACKS WITH VS. WITHOUT OUR AES.

Surrogate	Attack	Inc-v3 _{adv}	Inc-v3 _{ens3}	Inc-v3 _{ens4}	IncRes-v2 _{ens}	HGD	R&P	NIPS-r3	NRP	Bit-Red	Swin	AVG
Inc-v3	MI	27.2	22.2	22.4	11.2	8.2	10.7	12.6	16.1	26.4	26.4	18.3
	+AES-tune	31.7	26.8	28.5	15.2	16.1	14.2	15.5	17.7	26.5	27.8	22.0
	+AES-rand	32.1	26.4	27.0	14.1	14.4	13.5	15.5	16.5	26.7	27.6	21.4
	NI	27.8	23.1	23.1	11.7	8.3	11.3	13.6	16.8	26.6	30.2	19.3
	+AES-tune	35.9	29.8	30.9	16.2	18.1	15.9	19.0	16.6	27.9	32.0	24.2
	+AES-rand	36.0	30.0	29.7	15.6	17.0	14.7	18.3	16.8	27.9	32.9	23.9
	VMI	45.1	42.5	42.1	25.4	23.8	23.7	30.7	23.5	34.5	43.7	33.5
	+AES-tune	51.0	45.1	46.1	29.2	33.1	29.1	32.3	26.1	35.3	44.7	37.2
	+AES-rand	50.8	46.1	46.3	30.0	33.0	28.4	32.5	25.6	35.5	45.2	37.3
	PGN	71.4	65.4	64.5	45.5	38.5	46.0	53.2	44.8	52.9	62.3	54.5
	+AES-tune	75.5	71.2	74.1	56.8	62.9	54.3	60.1	48.3	56.2	59.3	61.9
	+AES-rand	76.1	71.2	74.7	56.5	62.4	54.5	60.3	48.0	56.6	58.2	61.9
Inc-v4	MI	25.3	19.8	18.5	11.9	8.3	10.4	12.4	14.7	23.9	29.3	17.5
	+AES-tune	27.9	23.5	24.0	13.3	14.7	14.1	13.7	15.5	25.8	30.3	20.3
	+AES-rand	27.6	23.5	23.9	12.7	13.1	13.6	13.5	14.9	24.4	31.8	19.9
	NI	24.4	19.6	18.9	11.1	7.7	10.2	12.2	14.5	25.2	30.9	17.5
	+AES-tune	27.8	25.3	25.4	14.3	17.5	14.6	16.3	14.3	25.9	32.4	21.4
	+AES-rand	26.0	23.7	23.7	12.9	15.1	12.9	14.9	15.2	26.4	33.9	20.5
	VMI	40.7	41.7	40.4	27.2	26.0	27.7	31.2	23.4	34.1	49.1	34.2
	+AES-tune	45.5	45.8	46.7	32.6	35.9	33.5	36.3	26.1	35.9	51.0	38.9
	+AES-rand	45.1	45.9	46.4	31.9	34.8	32.4	35.5	25.9	35.5	50.1	38.4
	PGN	65.6	67.1	64.3	49.0	38.7	48.1	55.3	46.6	54.2	70.9	56.0
	+AES-tune	69.8	71.1	70.5	60.4	63.6	56.9	60.3	51.1	55.8	64.2	62.4
	+AES-rand	71.2	71.5	71.5	59.6	62.9	56.7	60.6	50.1	55.2	64.4	62.4
IncRes-v2	MI	27.7	21.2	21.7	14.7	12.4	13.5	15.5	16.1	26.1	27.8	19.7
	+AES-tune	31.2	26.3	27.5	21.1	22.2	18.1	19.8	16.0	25.7	29.2	23.7
	+AES-rand	30.6	27.0	25.7	19.5	20.4	18.3	20.2	16.1	27.1	29.8	23.5
	NI	27.2	18.7	18.4	12.6	10.5	11.8	13.9	14.7	24.5	28.2	18.1
	+AES-tune	32.4	25.6	24.9	19.0	22.1	18.1	19.2	16.3	24.9	27.5	23.0
	+AES-rand	30.2	24.1	23.8	17.1	19.7	15.9	17.3	15.9	25.5	27.4	21.7
	VMI	47.2	48.7	44.5	37.5	36.0	34.9	37.5	23.8	35.4	47.4	39.3
	+AES-tune	53.4	54.7	50.5	46.7	47.8	42.6	44.0	26.9	37.2	48.5	45.2
	+AES-rand	53.3	53.7	50.7	47.4	47.9	42.3	43.9	27.0	37.1	48.1	45.1
	PGN	75.1	75.3	70.8	66.3	58.2	63.6	66.9	51.5	58.5	69.8	65.6
	+AES-tune	77.7	78.4	75.6	74.7	73.8	69.6	72.0	56.2	61.7	64.8	70.5
	+AES-rand	79.4	78.5	75.7	73.9	73.8	69.7	72.3	56.0	61.6	64.3	70.5
Res-152	MI	28.9	27.0	25.9	15.4	17.7	15.4	18.8	19.2	27.0	31.0	22.6
	+AES-tune	32.5	30.1	29.9	19.7	25.5	19.1	20.8	19.1	26.4	32.0	25.5
	+AES-rand	32.8	30.9	31.1	19.8	26.1	19.4	20.8	19.4	28.0	31.8	26.0
	NI	31.3	28.1	25.5	16.0	16.2	16.2	19.1	19.0	26.5	32.4	23.0
	+AES-tune	36.8	34.9	35.1	21.9	32.4	23.3	26.6	19.7	28.6	35.4	29.5
	+AES-rand	37.2	32.9	33.7	20.5	29.4	21.8	24.8	19.2	29.3	36.4	28.5
	VMI	45.4	46.6	43.1	32.5	38.4	32.3	37.3	27.2	35.7	47.2	38.6
	+AES-tune	50.6	51.1	47.6	37.3	44.6	36.9	42.0	29.1	36.3	48.5	42.4
	+AES-rand	49.9	50.6	47.7	36.0	44.0	36.2	41.3	29.4	36.4	48.1	42.0
	PGN	71.3	69.0	68.1	58.4	61.8	58.1	63.3	49.0	54.3	62.2	61.6
	+AES-tune	72.7	72.3	69.8	63.2	67.2	59.8	64.1	52.6	57.9	57.4	63.7
	+AES-rand	73.2	71.6	70.2	61.7	66.5	60.4	63.7	52.4	57.8	57.6	63.5
Ensemble	MI	42.4	43.0	40.9	27.5	33.3	26.8	33.3	23.5	34.1	54.5	35.9
	+AES-tune	52.5	53.3	50.9	36.1	51.4	36.0	41.0	24.7	34.2	58.8	43.9
	+AES-rand	51.2	52.5	49.9	35.3	47.6	34.9	39.5	24.7	34.6	59.4	43.0
	NI	44.5	44.8	41.0	26.6	29.1	27.3	32.3	24.4	34.2	57.4	36.2
	+AES-tune	62.9	60.2	57.4	42.7	57.1	42.3	47.7	25.1	34.8	64.5	49.5
	+AES-rand	58.8	56.0	53.1	38.6	48.8	37.4	43.1	25.4	36.2	63.2	46.1
	VMI	67.4	69.8	67.9	56.0	62.0	55.8	60.0	40.3	49.5	74.2	60.3
	+AES-tune	73.4	73.9	73.4	62.0	69.6	62.4	64.0	40.7	50.0	74.9	64.4
	+AES-rand	72.2	73.3	73.1	61.7	69.3	62.9	65.0	41.2	50.8	74.8	64.4
	PGN	88.8	89.2	88.1	82.7	84.0	83.1	85.6	74.2	78.7	89.6	84.4
	+AES-tune	90.9	90.3	89.8	86.4	89.2	85.9	87.6	78.5	79.8	87.9	86.6
	+AES-rand	91.0	90.5	89.4	86.3	89.3	85.9	87.0	78.7	79.1	88.0	86.5

stability, input transformation, and feature disruption. We consider the transferability settings with either a single surrogate model or an ensemble of surrogate models.

Based on the results from Table III to Table V, our AES

improves all the 10 attacks (from three categories) on 10 diverse target models in both the settings of single surrogate and ensemble surrogate. The improvement can be up to 13.3%, for ensemble transfer with AES-tune for gradient stability

TABLE IV
THE SUCCESS RATES (%) OF INPUT TRANSFORMATION ATTACKS WITH VS. WITHOUT OUR AES.

Surrogate	Attack	Inc-v3 _{adv}	Inc-v3 _{ens3}	Inc-v3 _{ens4}	IncRes-v2 _{ens}	HGD	R&P	NIPS-r3	NRP	Bit-Red	Swin	AVG
Inc-v3	DIM	36.0	31.8	30.9	16.6	16.0	16.6	22.0	18.5	30.7	38.3	25.7
	+AES-tune	49.3	45.8	47.2	28.8	39.1	31.0	35.5	21.8	32.3	42.1	37.3
	+AES-rand	47.4	45.8	47.4	28.7	39.4	31.1	34.3	20.8	32.6	41.8	36.9
	SIM	46.4	39.4	38.6	22.9	20.1	21.4	27.5	25.6	37.8	41.3	32.1
	+AES-tune	56.2	47.5	47.9	29.6	35.8	28.1	36.0	27.1	38.3	42.2	38.9
	+AES-rand	54.5	45.6	45.8	28.1	31.7	26.9	33.0	26.5	38.6	41.8	37.3
	Admix	50.2	45.3	45.4	27.0	24.9	25.4	33.0	30.3	40.9	46.3	36.9
	+AES-tune	62.8	55.5	56.4	37.9	47.5	37.8	42.4	31.3	44.2	47.4	46.3
	+AES-rand	62.0	57.4	57.9	38.5	49.3	38.3	42.8	31.8	44.2	48.6	47.1
	SSA	64.3	56.6	55.8	35.4	32.9	36.3	42.6	34.3	45.4	56.0	46.0
	+AES-tune	71.7	67.4	67.7	49.9	59.9	48.6	54.8	40.1	48.9	56.1	56.5
	+AES-rand	71.6	67.4	67.4	49.9	59.7	48.5	54.4	39.4	47.9	56.4	56.3
Inc-v4	DIM	28.7	26.1	25.8	15.8	16.3	16.8	19.2	16.5	27.0	38.6	23.1
	+AES-tune	38.3	39.9	38.5	27.7	37.2	29.0	28.8	18.4	28.9	44.8	33.2
	+AES-rand	37.1	38.6	38.8	26.4	36.7	28.4	30.0	17.6	30.0	45.0	32.9
	SIM	45.8	47.7	42.8	28.8	26.4	27.7	33.6	24.1	37.9	51.2	36.6
	+AES-tune	55.3	56.6	53.3	37.6	44.0	38.4	43.1	25.9	40.2	54.2	44.9
	+AES-rand	53.6	55.6	52.3	35.9	37.8	36.3	39.5	26.9	40.3	55.7	43.4
	Admix	50.8	53.5	49.5	32.6	33.7	33.0	39.6	29.5	41.4	56.9	42.1
	+AES-tune	59.4	64.0	61.7	46.8	56.7	47.2	52.2	31.8	43.5	58.8	52.2
	+AES-rand	60.8	62.2	60.6	45.2	55.2	45.8	51.6	31.4	43.7	56.2	51.3
	SSA	59.5	57.1	55.6	36.0	30.8	37.9	44.7	35.1	44.6	64.2	46.6
	+AES-tune	66.2	66.8	65.4	50.0	58.9	51.5	54.6	41.0	48.8	61.3	56.5
	+AES-rand	65.6	66.7	66.1	51.4	59.6	52.2	56.5	41.2	47.5	61.1	56.8
IncRes-v2	DIM	34.6	33.7	31.7	22.1	21.2	22.2	23.6	18.8	28.7	38.2	27.5
	+AES-tune	41.0	42.0	38.9	37.0	39.2	35.8	36.6	19.2	29.2	38.6	35.8
	+AES-rand	40.8	41.8	39.5	37.0	38.9	35.2	37.0	19.0	29.2	38.4	35.7
	SIM	57.0	56.5	47.9	39.4	38.1	37.5	41.6	29.9	42.3	46.4	43.7
	+AES-tune	67.4	64.7	58.0	54.1	59.9	50.0	53.3	32.0	44.5	49.6	53.4
	+AES-rand	65.5	63.5	55.6	51.0	53.3	46.2	50.0	31.9	43.2	48.1	50.8
	Admix	66.5	68.9	62.3	52.7	52.9	49.7	54.7	37.1	50.8	57.4	55.3
	+AES-tune	77.2	75.4	71.9	68.9	73.3	65.2	68.2	40.4	51.4	59.9	65.2
	+AES-rand	75.3	75.4	69.4	66.9	70.7	63.2	66.4	39.7	50.4	57.7	63.5
	SSA	67.2	67.6	61.7	55.1	56.3	54.2	58.0	38.8	49.5	63.7	57.2
	+AES-tune	73.6	73.1	69.6	68.1	69.2	63.7	66.0	43.3	53.6	61.9	64.2
	+AES-rand	73.9	73.4	69.3	67.4	70.1	63.6	66.2	44.9	53.4	60.9	64.3
Res-152	DIM	41.0	42.4	40.0	25.8	34.4	26.4	31.3	23.8	34.3	45.4	34.5
	+AES-tune	53.6	56.6	52.8	42.7	54.3	45.4	48.4	25.4	38.3	50.4	46.8
	+AES-rand	52.8	54.9	51.9	42.7	53.9	45.0	47.1	25.2	37.0	50.1	46.1
	SIM	47.7	45.6	43.3	29.3	33.0	29.6	34.2	28.5	37.4	44.9	37.4
	+AES-tune	56.9	55.1	51.5	38.7	49.8	39.5	44.6	28.3	39.5	46.3	45.0
	+AES-rand	56.8	52.8	50.5	36.1	44.5	36.3	42.0	29.2	39.7	45.9	43.4
	Admix	45.9	47.2	43.3	31.3	35.9	30.8	36.2	30.5	39.1	45.1	38.5
	+AES-tune	56.9	56.5	54.3	44.3	53.9	42.1	49.1	31.9	41.7	49.2	48.0
	+AES-rand	55.0	54.6	52.7	43.3	52.8	40.6	46.9	31.2	40.3	48.5	46.6
	SSA	66.2	63.0	60.2	45.5	54.7	47.6	54.2	41.2	49.2	59.6	54.1
	+AES-tune	70.2	68.1	66.1	58.1	67.5	57.6	61.8	45.9	52.5	57.4	60.5
	+AES-rand	69.5	68.4	65.9	58.4	67.3	56.9	60.7	45.1	52.2	58.7	60.3
Ensemble	DIM	63.7	72.2	67.1	53.0	63.0	57.1	62.7	36.1	49.0	74.5	59.8
	+AES-tune	81.9	82.6	80.0	73.6	81.6	76.4	76.9	39.7	53.4	78.3	72.4
	+AES-rand	80.8	82.9	79.4	74.3	81.7	76.6	77.4	40.6	55.3	78.1	72.7
	SIM	76.5	79.1	76.0	58.7	65.9	59.9	66.4	46.5	57.8	79.6	66.6
	+AES-tune	87.4	87.0	85.3	73.4	85.9	75.4	80.6	47.6	61.0	83.2	76.7
	+AES-rand	84.9	86.5	83.4	68.5	80.3	69.9	76.6	47.7	60.4	82.6	74.1
	Admix	74.5	80.3	78.1	64.1	74.1	63.9	69.6	46.9	58.1	80.2	69.0
	+AES-tune	84.0	86.0	84.4	75.4	84.5	75.2	78.8	49.8	61.1	82.1	76.1
	+AES-rand	80.2	83.8	81.8	70.5	81.3	70.7	75.3	47.2	59.5	81.6	73.2
	SSA	89.3	88.9	85.8	77.1	81.3	80.1	83.7	62.6	72.4	89.9	81.1
	+AES-tune	91.4	90.7	89.4	85.6	90.7	86.7	88.4	72.2	75.6	88.0	85.9
	+AES-rand	91.6	91.0	89.5	85.9	91.2	86.8	88.7	71.2	76.0	88.8	86.1

attacks. As expected, the results of ensemble transfer are generally better than those of the single transfer, but at the cost of more time and computations. Note that for the ensemble surrogate transfer, we follow the common practice [25] to

combine the logit outputs of different models, here, Inc-v3, Inc-v4, InRes-v2, and Res-152.

In particular, we notice that the improvement on Swin is relatively small, suggesting that transferring to a different

TABLE V
THE SUCCESS RATES (%) OF FEATURE DISRUPTION ATTACKS WITH VS. WITHOUT OUR AES.

Surrogate	Attack	Inc-v3 _{adv}	Inc-v3 _{ens3}	Inc-v3 _{ens4}	IncRes-v2 _{ens}	HGD	R&P	NIPS-r3	NRP	Bit-Red	Swin	AVG
Inc-v3	FIA	53.3	35.8	35.5	20.9	10.5	19.0	25.6	24.4	40.9	46.3	31.2
	+AES-tune	59.8	47.3	46.8	30.7	33.0	29.6	36.3	26.2	44.4	47.3	40.1
	+AES-rand	59.0	45.0	44.7	29.2	31.3	28.7	35.0	25.0	44.5	46.6	38.9
	NAA	63.7	52.5	50.6	32.6	20.4	33.1	40.0	33.5	47.1	58.2	43.2
	+AES-tune	69.5	60.4	60.8	45.3	49.3	44.7	50.1	37.5	49.9	58.3	52.6
	+AES-rand	69.6	61.0	60.8	46.8	49.9	46.2	50.2	38.4	49.9	58.3	53.1
Inc-v4	FIA	45.1	38.4	36.7	20.5	16.7	21.2	27.4	23.4	39.1	54.7	32.3
	+AES-tune	55.3	49.6	47.7	29.9	37.1	31.9	37.8	24.9	42.2	54.3	41.1
	+AES-rand	54.4	49.1	46.7	29.2	36.9	30.4	36.6	25.5	41.1	54.4	40.4
	NAA	53.3	51.8	47.3	32.2	28.8	31.6	37.5	31.2	43.7	63.5	42.1
	+AES-tune	61.0	59.0	58.0	43.9	51.1	44.3	49.2	32.0	44.2	63.3	50.6
	+AES-rand	60.8	58.3	57.5	43.3	51.4	43.9	48.5	32.4	44.5	64.1	50.5
IncRes-v2	FIA	63.5	50.6	45.0	34.7	23.4	31.2	40.5	29.5	50.8	47.4	41.7
	+AES-tune	62.6	56.0	53.1	45.4	48.2	41.3	47.9	31.7	51.4	46.8	48.4
	+AES-rand	62.0	55.0	53.0	45.1	46.9	40.3	46.7	30.7	50.4	46.7	47.7
	NAA	64.4	59.3	55.9	51.0	38.0	46.8	51.0	40.2	50.9	57.4	51.5
	+AES-tune	65.8	64.0	60.5	58.6	57.4	55.6	56.5	43.2	53.9	55.7	57.1
	+AES-rand	65.8	64.2	61.0	59.3	59.5	55.5	57.2	42.8	52.0	56.1	57.3
Res-152	FIA	57.9	48.9	43.8	28.4	33.8	30.8	36.8	28.9	46.9	50.5	40.7
	+AES-tune	65.6	58.8	56.9	44.7	54.0	43.3	50.2	30.8	47.5	52.0	50.4
	+AES-rand	65.7	59.1	56.1	43.6	53.6	42.6	48.5	31.0	48.2	50.6	49.9
	NAA	65.6	61.4	57.6	47.1	49.9	48.3	53.1	39.2	49.8	63.1	53.5
	+AES-tune	71.8	68.5	66.0	58.0	66.6	57.8	62.3	42.7	52.7	63.0	60.9
	+AES-rand	72.0	69.0	66.1	57.7	67.8	58.7	62.7	42.6	53.0	63.4	61.3

TABLE VI

DIVERSITY OF SUCCESS RATES FOR DIFFERENT ATTACKS. GRADIENT STABILITY ATTACKS YIELD THE LOWEST DIVERSITY, REPRESENTED BY THE LOWEST STANDARD DEVIATIONS. AES-RAND ON INC-V3 IS USED.

Attack	Inc-v3 _{adv}	Inc-v3 _{ens3}	Inc-v3 _{ens4}	IncRes-v2 _{ens}
MI	27.1(±0.62)	22.6(±0.58)	22.2(±0.37)	11.3(±0.25)
NI	28.3(±0.66)	22.5(±0.44)	22.5(±0.57)	11.4(±0.42)
VMI	45.1(±0.37)	41.5(±0.47)	41.3(±0.41)	24.9(±0.42)
PGN	70.5(±0.67)	64.9(±0.58)	65.7(±0.68)	45.2(±0.64)
DIM	35.4(±0.59)	31.7(± 1.18)	31.4(± 0.86)	17.0(±0.66)
SIM	46.5(±0.59)	39.3(±0.52)	38.2(±0.40)	23.1(±0.51)
Admix	52.1(±0.43)	45.9(±0.72)	45.2(±0.69)	26.9(±0.45)
SSA	63.0(± 0.69)	56.4(±0.50)	56.3(±0.67)	35.2(±0.74)
FIA	54.2(±0.65)	35.8(±0.50)	35.4(±0.50)	19.8(±0.69)
NAA	63.5(±0.51)	52.0(±0.83)	51.7(±0.58)	32.5(± 0.78)

architecture is difficult. This is consistent with the previous finding that changing the model architecture is normally more effective than applying a defense [19]. In almost all cases, AES-tune slightly outperforms AES-rand. This may be because the change of the hyperparameter is normally larger than that in repeated experiments (with the same hyperparameter).

When comparing the three attack categories, we can observe that the improvement for gradient stability attacks under single model setting is the smallest, *i.e.*, 1.9%-7.4% for gradient stability vs. 5.2%-12.3% for input transformation vs. 5.6%-9.9% for feature disruption. This may be because the hyperparameter tuning for gradient stability attacks yields the least diverse results. The results in Table VI support our explanation, where gradient stability attacks yield the smallest fluctuation of transferability across different sessions of hyperparameters. In addition, we notice that in a few cases involving the PGN attack, AES even decreases the transferability, which is worth

TABLE VII

THE STEALTHINESS OF DIFFERENT ATTACKS WITH OR WITHOUT OUR AES. THE SURROGATE MODEL IS INC-V3.

Attack	PSNR↑	SSIM↑	LPIPS↓	FID↓
MI	26.954	0.6691	0.1348	83.858
+AES-tune	28.643	0.7441	0.1038	77.102
+AES-rand	27.892	0.7219	0.1154	78.732
NI	26.921	0.6653	0.1385	98.459
+AES-tune	29.261	0.7594	0.0985	84.759
+AES-rand	28.360	0.7235	0.1121	88.527
VMI	27.090	0.6840	0.1262	96.902
+AES-tune	27.627	0.7103	0.1166	93.024
+AES-rand	27.655	0.7125	0.1151	92.519
PGN	26.630	0.6730	0.1272	115.034
+AES-tune	29.934	0.8489	0.0659	101.437
+AES-rand	29.935	0.8490	0.0660	99.778
DIM	26.920	0.6686	0.1330	95.472
+AES-tune	31.944	0.8501	0.0605	69.973
+AES-rand	32.161	0.8566	0.0581	67.438
SIM	26.879	0.6688	0.1357	112.549
+AES-tune	28.649	0.7507	0.1042	104.025
+AES-rand	27.952	0.7218	0.1156	106.001
Admix	26.825	0.6697	0.1336	115.356
+AES-tune	29.624	0.8077	0.0814	99.651
+AES-rand	29.722	0.8123	0.0801	97.342
SSA	26.701	0.6628	0.1298	110.153
+AES-tune	30.380	0.8507	0.0639	93.475
+AES-rand	30.323	0.8493	0.0642	91.640
FIA	26.560	0.6692	0.1369	136.777
+AES-tune	28.748	0.7711	0.1016	126.076
+AES-rand	28.747	0.7713	0.1017	125.552
NAA	26.545	0.6698	0.1369	123.369
+AES-tune	28.990	0.7849	0.0941	111.337
+AES-rand	29.001	0.7853	0.0943	108.836

more in-depth exploration in the future.

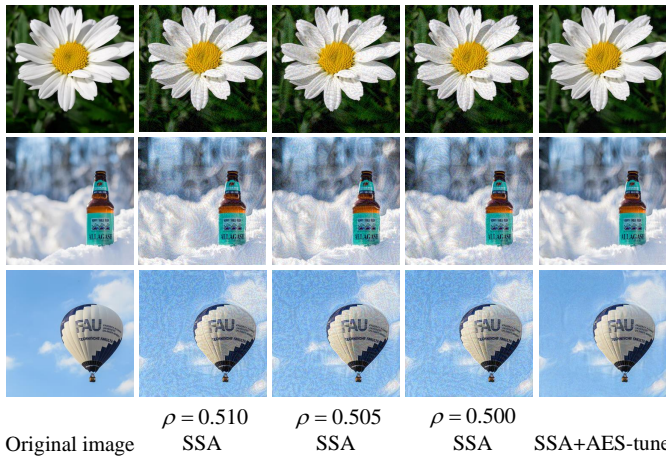


Fig. 3. Visualizations of adversarial images generated by SSA with different hyperparameters vs. our AES. AES leads to higher image quality.

C. AES Improves Stealthiness

Since AES takes the average of adversarial examples, it may cancel out specific pixel perturbations that are unstable across different sessions. This suggests that AES may naturally lead to less noisy images, *i.e.*, improving the attack stealthiness. To validate this, we evaluate the visual quality of the adversarial images generated by AES using four popular metrics: Peak Signal-to-Noise Ratio (PSNR) [19], Structural Similarity Index Measure (SSIM) [60], Learned Perceptual Image Patch Similarity (LPIPS) [61] and Frechet Inception Distance (FID) [57]. As shown in Table VII, both AES-tune and AES-rand substantially outperform the baseline attacks in all metrics. For example, in terms of the FID metric, DIM+AES-tune achieves the best FID score of 69.973, while DIM only achieves 95.472. The visualizations in Figure 3 further confirm that our AES leads to higher visual quality of the adversarial images. In general, it is surprising that our AES can simultaneously improve transferability and stealthiness since most existing transferable attacks have to trade off these two properties [19].

We further understand the perturbation averaging from the perspective of model attention. To this end, we visualize the CAM [62] attention map of a Res-50 classifier for clean vs. adversarial images, with their top-1 predicted label, *i.e.*, correct labels for original images and incorrect labels for the adversarial images. As shown in Figure 4, different hyperparameters of the Admix attack lead to attention maps that spread different local regions with a large overlap around the object. After our AES is applied, the attention map becomes more concentrated, indicating that our AES cancels out unstable perturbations towards improved attack stealthiness, *i.e.*, image quality. In addition, the concentrate attention map of AES is distant from the object, validating its effectiveness in improving attack success, *i.e.*, transferability.

D. Ablation Studies

In this subsection, we conduct detailed ablation studies to explore the impact of hyperparameters of AES on its performance.

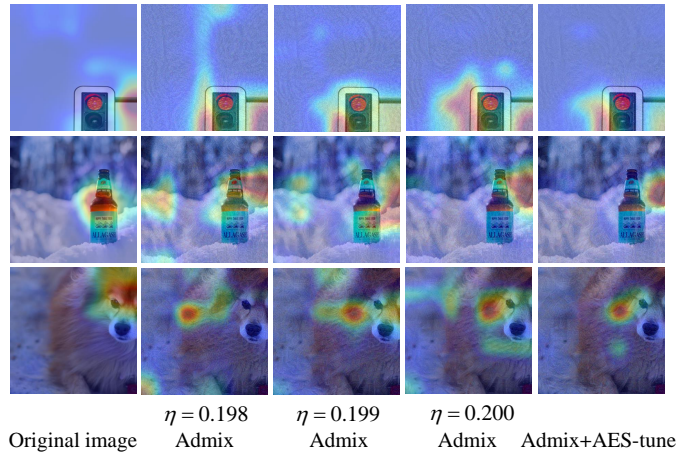
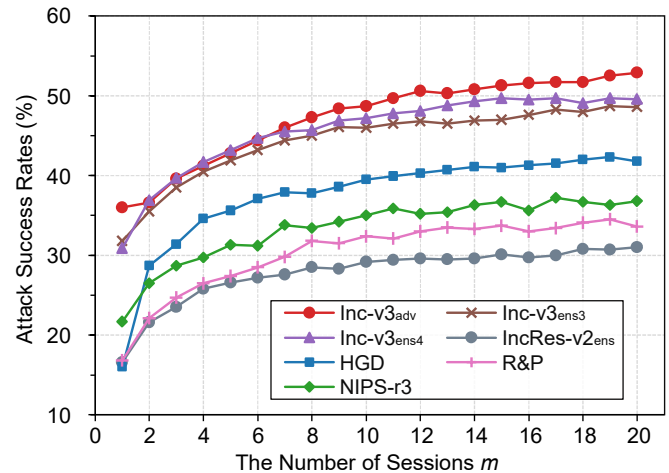
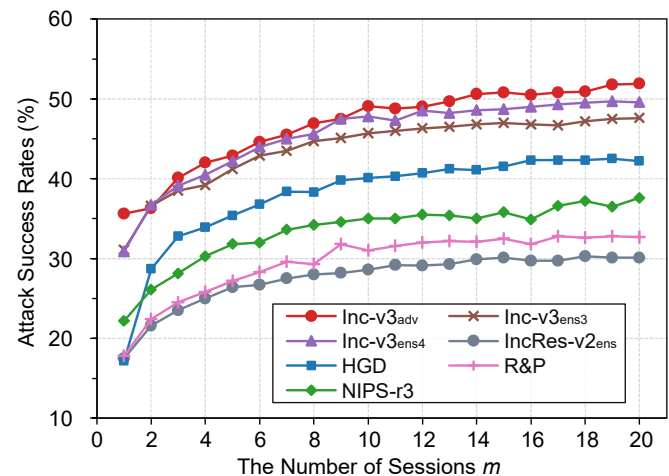


Fig. 4. CAM attentions of adversarial images generated by Admix with different hyperparameters vs. AES. AES leads to a more concentrated attention region, which is also distant from the correct object region.



(a) AES-tune



(b) AES-rand

Fig. 5. Ablation study on the number of sessions m . The surrogate model is Inc-v3.

The number of sessions m . We use DIM as the baseline attack and generate adversarial examples on Inc-v3. The

TABLE VIII
THE SUCCESS RATES (%) OF AES FOR INTEGRATED ATTACKS. THE SURROGATE MODEL IS INC-V3.

Attack	Inc-v3 _{adv}	Inc-v3 _{ens3}	Inc-v3 _{ens4}	IncRes-v2 _{ens}	HGD	R&P	NIPS-r3	NRP	Bit-Red	Swin	AVG
TI-DIM	45.9	48.2	46.7	32.8	39.5	34.2	38.2	25.7	38.5	39.9	39.0
+AES-tune	56.8	54.5	54.5	37.4	42.1	41.4	44.2	27.6	40.0	39.5	43.8
+AES-rand	56.9	54.9	53.6	39.7	43.9	40.0	43.4	26.7	38.6	41.9	44.0
SI-NI-DIM	52.3	47.0	45.0	28.7	26.8	27.6	36.7	28.0	42.1	49.2	38.3
+AES-tune	58.1	56.8	57.1	40.8	48.0	40.6	45.5	30.7	42.2	45.5	46.5
+AES-rand	60.1	57.5	56.7	41.3	49.5	41.3	46.4	32.5	42.7	47.0	47.5
SSA-SI-DIM	85.4	83.7	81.9	66.0	72.1	70.3	75.4	55.2	67.2	72.4	73.0
+AES-tune	88.8	86.9	85.4	74.8	80.2	76.3	80.3	59.8	68.4	72.0	77.3
+AES-rand	88.7	86.8	85.2	74.3	80.6	77.8	80.3	60.2	70.2	72.7	77.7
PGN-DIM	77.7	75.8	75.3	58.4	56.2	61.3	66.9	53.5	63.0	74.2	66.2
+AES-tune	82.4	80.4	80.3	68.0	75.2	66.9	72.8	58.0	64.9	68.2	71.7
+AES-rand	81.6	80.4	80.8	68.2	74.9	67.4	71.5	59.0	64.2	68.4	71.6

number of sessions m ranges from 1 to 20. When $m = 1$, AES is equivalent to the naive DIM. As shown in Figure 5a and 5b, for both AES-tune and AES-rand, the transferability gradually increases as m increases, and it becomes almost saturated after $m > 10$. It should be noted that a larger m means a higher cost of time and computations. In our main experiments, we set $m = 10$ for a good trade-off between transferability and cost. In this case, the averaging operation on each image only costs 0.036s.

Averaging strategy. We consider three widely used averaging strategies: uniform, weighted, and greedy. Different from the uniform strategy in our main experiments, both the weighted and greedy strategies assign weights to adversarial examples in different sessions. Here we use VMI since its hyperparameter, *i.e.*, the number of copies N , is an integer. Therefore, it is straightforward to determine the weights of different adversarial images according to N . Specifically, we vary N from 16 to 25 to generate 10 sessions of adversarial examples on Inc-v3. For the weighted strategy, the weights are determined by ranking the transferability of the 10 sessions of adversarial examples on Inc-v4, with the best-performed one assigned a weight of 25/205 and the worst assigned 16/205. For the greedy strategy, only the top-5 adversarial examples according to the above ranking are used for averaging. For a fair comparison and because the number of sessions has a significant impact on the performance, we still use 10 sessions, with the rest 5 sessions randomly chosen from the original 10 sessions for $N = 20$. The results in Table IX demonstrates that all three averaging strategies substantially improve transferability, with the greedy strategy achieving slightly better results than the other two. Since the uniform averaging strategy does not require weighting allocation and sample selection, it is more simple and efficient, so we mainly adopt this averaging method for AES. Naturally, we can also choose different averaging methods according to actual circumstances.

V. FURTHER ANALYSIS AND DISCUSSION

A. AES for Integrated Attacks

In practice, different (categories of) transferable attacks can be integrated to achieve higher transferability. To shed

TABLE IX
ABLATION STUDY ON THE THREE AVERAGING STRATEGIES: UNIFORM, WEIGHTED, AND GREEDY. THE SURROGATE MODEL IS INC-V3.

VMI	Inc-v3 _{adv}	Inc-v3 _{ens3}	Inc-v3 _{ens4}	IncRes-v2 _{ens}	AVG
N=16	44.7	41.8	40.9	24.5	38.0
N=17	45.5	40.3	40.6	24.6	37.8
N=18	44.5	41.2	40.8	23.5	37.5
N=19	44.9	41.3	41.8	24.6	38.2
N=20	45.2	41.9	40.2	25.0	38.1
N=21	45.2	41.1	42.5	24.7	38.4
N=22	45.3	42.3	41.7	25.2	38.6
N=23	45.3	41.3	41.3	25.0	38.2
N=24	44.3	41.4	41.2	25.2	38.0
N=25	44.5	41.4	41.1	25.6	38.2
Uniform	51.0	45.1	46.1	29.2	42.9
Weighted	51.1	45.1	45.8	29.2	42.8
Greedy	51.9	46.3	47.9	30.0	44.0

light on the practical usefulness of AES, we evaluate it in such integrated scenarios, involving two categories of attacks: gradient stability and input transformation. Since the integrated attacks contain multiple basic attacks, multiple hyperparameters can be tuned. In our case, for AES-tune, we only tune the hyperparameter of one basic attack and keep the rest fixed. Specifically, TI-DIM adjusts hyperparameter in DIM, SI-NI-DIM in SIM, SSA-SI-DIM in SSA, and PGN-DIM in PGN. The specific details are shown in Table II. For AES-rand, the optimization is repeated multiple times as done in our main experiments. As shown in Table VIII, our AES achieves the highest average transferability in all cases.

B. AES in the Wild

In the previous experiments, we focus on AES from the perspective of attack optimization, involving two common operations: hyperparameter tuning and stability testing. There may also be other types of AES, as long as the underlying assumption of “multiple adversarial examples lie in the same error basin” is satisfied. A promising type of AES in the real world is that we could leverage in-the-wild adversarial images to boost their transferability and stealthiness. This is possible considering that the source code for implementing different attacks is publicly available, and different kinds of adversarial images may be visualized anywhere.

TABLE X

THE SUCCESS RATES (%) OF AES IN THE WILD THAT DIRECTLY AVERAGES ADVERSARIAL IMAGES FROM TWO ATTACKS. THE SURROGATE MODEL IS AN ENSEMBLE OF INC-V3, INC-V4, INCRES-V2, AND RES-152.

Attack	Inc-v3 _{adv}	Inc-v3 _{ens3}	Inc-v3 _{ens4}	IncRes-v2 _{ens}	HGD	R&P	NIPS-r3	NRP	Bit-Red	Swin	AVG
MI	42.6	42.8	40.8	26.4	33.3	26.8	33.3	22.7	33.9	56.0	35.9
NI	45.5	45.5	39.6	27.3	29.1	27.3	32.3	23.1	35.1	57.7	36.3
AES-MI&NI	49.6	53.3	49.2	37.8	50.4	35.6	40.2	26.6	35.0	61.8	44.0
SIM	76.2	79.2	75.3	58.3	65.9	59.9	66.4	45.7	58.0	79.9	66.5
Admix	75.2	81.3	77.7	64.0	74.1	63.9	69.6	46.0	57.8	79.8	68.9
AES-SIM&Admix	79.3	84.7	81.7	70.5	82.0	70.7	72.5	50.9	60.9	81.5	73.5

TABLE XI

THE STEALTHINESS OF AES IN THE WILD THAT DIRECTLY AVERAGES ADVERSARIAL IMAGES FROM TWO ATTACKS. THE SURROGATE MODEL IS AN ENSEMBLE OF INC-V3, INC-V4, INCRES-V2, AND RES-152.

Attack	PSNR \uparrow	SSIM \uparrow	LPIPS \downarrow	FID \downarrow
MI	27.025	0.6717	0.1360	85.810
NI	26.922	0.6648	0.1425	88.191
AES-MI&NI	28.406	0.7262	0.1110	79.572
SIM	26.851	0.6672	0.1349	108.315
Admix	26.905	0.6734	0.1299	104.881
AES-SIM&Admix	28.338	0.7345	0.1054	97.248

To validate the effectiveness of our AES in this scenario, we try directly averaging the adversarial examples from different attacks. To this end, we select the adversarial examples from attacks that yield similar transferability on a hold-out target model. Note that this selection can also be conducted at the sample level, by selecting the adversarial examples that yield similar loss values. As shown in Table X and XI, AES for the pair of MI and NI or SIM and Admix consistently improves the transferability and stealthiness.

VI. CONCLUSIONS

In this paper, we question the common recipe for optimizing transferability, which directly discards the adversarial examples obtained during the optimization process. Specifically, we propose Adversarial Example Soups (AES), which reuses discarded adversarial examples for improved transferability and stealthiness. We demonstrate the global effectiveness of AES in boosting 10 state-of-the-art transferable attacks and their combinations against 10 diverse (defensive) target models. We also find that AES improves stealthiness since the perturbation variances are naturally reduced. Beyond optimization, we discuss other types of AES, *e.g.*, averaging multiple in-the-wild adversarial examples that yield comparable success to boost their transferability. In the future, it would be promising to generalize the paradigm of AES to more types or other domains, such as text and speech.

VII. ACKNOWLEDGEMENT

This research is supported by the National Key Research and Development Program of China (2023YFB3107400), the National Natural Science Foundation of China (62376210, 62161160337, 62132011, U21B2018, U20A20177, U20B2049 and 62006181).

REFERENCES

- [1] K. Simonyan and A. Zisserman, "Very deep convolutional networks for large-scale image recognition," in *International Conference on Learning Representations (ICLR)*, 2015.
- [2] K. He, X. Zhang, S. Ren, and J. Sun, "Deep residual learning for image recognition," in *Proceedings of the IEEE Conference on Computer Vision and Pattern Recognition (CVPR)*, 2016, pp. 770–778.
- [3] Y. Wen, K. Zhang, Z. Li, and Y. Qiao, "A discriminative feature learning approach for deep face recognition," in *European Conference on Computer Vision*, 2016.
- [4] H. Wang, Y. Wang, Z. Zhou, X. Ji, D. Gong, J. Zhou, Z. Li, and W. Liu, "Cosface: Large Margin Cosine Loss for Deep Face Recognition," in *Proceedings of the IEEE Conference on Computer Vision and Pattern Recognition (CVPR)*, 2018.
- [5] S. Ren, K. He, R. B. Girshick, and J. Sun, "Faster r-cnn: Towards real-time object detection with region proposal networks," *IEEE Transactions on Pattern Analysis and Machine Intelligence*, vol. 39, pp. 1137–1149, 2015.
- [6] J. Redmon, S. K. Divvala, R. B. Girshick, and A. Farhadi, "You only look once: Unified, real-time object detection," in *Proceedings of the IEEE Conference on Computer Vision and Pattern Recognition (CVPR)*, 2015, pp. 779–788.
- [7] C. Szegedy, W. Zaremba, I. Sutskever, J. Bruna, D. Erhan, I. Goodfellow, and R. Fergus, "Intriguing properties of neural networks," in *International Conference on Learning Representations (ICLR)*, 2014.
- [8] I. J. Goodfellow, J. Shlens, and C. Szegedy, "Explaining and harnessing adversarial examples," in *International Conference on Learning Representations (ICLR)*, 2015.
- [9] Y. Liu, X. Chen, C. Liu, and D. Song, "Delving into transferable adversarial examples and black-box attacks," in *International Conference on Learning Representations (ICLR)*, 2017.
- [10] N. Carlini and D. Wagner, "Towards evaluating the robustness of neural networks," in *IEEE Symposium on Security and Privacy (S&P)*, 2017, pp. 39–57.
- [11] A. Madry, A. Makelov, L. Schmidt, D. Tsipras, and A. Vladu, "Towards deep learning models resistant to adversarial attacks," in *International Conference on Learning Representations (ICLR)*, 2018.
- [12] W. Wu, Y. Su, M. R. Lyu, and I. King, "Improving the transferability of adversarial samples with adversarial transformations," *2021 IEEE/CVF Conference on Computer Vision and Pattern Recognition (CVPR)*, pp. 9020–9029, 2021.
- [13] Z. Zhao, Z. Liu, and M. Larson, "Adversarial image color transformations in explicit color filter space," *IEEE Transactions on Information Forensics and Security*, 2023.
- [14] Y. Xiong, J. Lin, M. Zhang, J. E. Hopcroft, and K. He, "Stochastic variance reduced ensemble adversarial attack for boosting the adversarial transferability," *2022 IEEE/CVF Conference on Computer Vision and Pattern Recognition (CVPR)*, pp. 14963–14972, 2021.
- [15] J. Zhang, J. tse Huang, W. Wang, Y. Li, W. Wu, X. Wang, Y. Su, and M. R. Lyu, "Improving the transferability of adversarial samples by path-augmented method," *2023 IEEE/CVF Conference on Computer Vision and Pattern Recognition (CVPR)*, pp. 8173–8182, 2023.
- [16] Z. Qin, Y. Fan, Y. Liu, L. Shen, Y. Zhang, J. Wang, and B. Wu, "Boosting the transferability of adversarial attacks with reverse adversarial perturbation," *In Advances in neural information processing systems*, 2022.
- [17] C. Xie, Z. Zhang, Y. Zhou, S. Bai, J. Wang, Z. Ren, and A. L. Yuille, "Improving transferability of adversarial examples with input diversity," in *Proceedings of the IEEE Conference on Computer Vision and Pattern Recognition (CVPR)*, 2019, pp. 2730–2739.

- [18] K. Liang and B. Xiao, "Styleless: Boosting the transferability of adversarial examples," *2023 IEEE/CVF Conference on Computer Vision and Pattern Recognition (CVPR)*, pp. 8163–8172, 2023.
- [19] Z. Zhao, H. Zhang, R. Li, R. Sicre, L. Amsaleg, M. Backes, Q. Li, and C. Shen, "Revisiting transferable adversarial image examples: Attack categorization, evaluation guidelines, and new insights," *arXiv preprint arXiv:2310.11850*, 2023.
- [20] Y. Yang, C. Lin, Q. Li, Z. Zhao, H. Fan, D. Zhou, N. Wang, T. Liu, and C. Shen, "Quantization aware attack: Enhancing transferable adversarial attacks by model quantization," *IEEE Transactions on Information Forensics and Security*, 2024.
- [21] J. Weng, Z. Luo, D. Lin, S. Li, and Z. Zhong, "Boosting adversarial transferability via fusing logits of top-1 decomposed feature," *ArXiv*, vol. abs/2305.01361, 2023.
- [22] Y. Zhu, J. Sun, and Z. Li, "Rethinking adversarial transferability from a data distribution perspective," in *International Conference on Learning Representations (ICLR)*, 2022.
- [23] Z. Zhao, Z. Liu, and M. Larson, "On success and simplicity: A second look at transferable targeted attacks," in *NeurIPS*, 2021.
- [24] Z. Liu, Z. Zhao, and M. Larson, "Who's afraid of adversarial queries? the impact of image modifications on content-based image retrieval," in *ICMR*, 2019.
- [25] Y. Dong, F. Liao, T. Pang, H. Su, J. Zhu, X. Hu, and J. Li, "Boosting adversarial attacks with momentum," in *Proceedings of the IEEE Conference on Computer Vision and Pattern Recognition (CVPR)*, 2018, pp. 9185–9193.
- [26] J. Lin, C. Song, K. He, L. Wang, and J. E. Hopcroft, "Nesterov Accelerated Gradient and Scale Invariance for Adversarial Attacks," in *International Conference on Learning Representations (ICLR)*, 2020.
- [27] Y. Dong, T. Pang, H. Su, and J. Zhu, "Evading Defenses to Transferable Adversarial Examples by Translation-invariant Attacks," in *Proceedings of the IEEE Conference on Computer Vision and Pattern Recognition (CVPR)*, 2019, pp. 4312–4321.
- [28] X. Wang, Z. Zhang, and J. Zhang, "Structure invariant transformation for better adversarial transferability," *ArXiv*, vol. abs/2309.14700, 2023.
- [29] Z. Wang, H. Guo, Z. Zhang, W. Liu, Z. Qin, and K. Ren, "Feature Importance-aware Transferable Adversarial Attacks," in *Proceedings of the IEEE Conference on Computer Vision and Pattern Recognition (CVPR)*, 2021, pp. 7639–7648.
- [30] J. Zhang, W. Wu, J. tse Huang, Y. Huang, W. Wang, Y. Su, and M. R. Lyu, "Improving adversarial transferability via neuron attribution-based attacks," *2022 IEEE/CVF Conference on Computer Vision and Pattern Recognition (CVPR)*, pp. 14 973–14 982, 2022.
- [31] Z. Ge, F. Shang, H. Liu, Y. Liu, and X. Wang, "Boosting adversarial transferability by achieving flat local maxima," in *Advances in Neural Information Processing Systems*, 2023.
- [32] Y. Zhang, S. Hu, L. Y. Zhang, J. Shi, M. Li, X. Liu, W. Wan, and H. Jin, "Why does little robustness help? a further step towards understanding adversarial transferability," in *2024 IEEE Symposium on Security and Privacy (SP)*. IEEE Computer Society, 2023, pp. 10–10.
- [33] X. Wang, J. Ren, S. Lin, X. Zhu, Y. Wang, and Q. Zhang, "A unified approach to interpreting and boosting adversarial transferability," in *International Conference on Learning Representations*, 2020.
- [34] G. I. Mitchell Wortsman, S. Y. Gadre, R. Roelofs, R. G. Lopes, A. S. Morcos, H. Namkoong, A. Farhadi, Y. Carmon, S. Kornblith, and L. Schmidt, "Model soups: averaging weights of multiple fine-tuned models improves accuracy without increasing inference time," in *International Conference on Machine Learning (ICML)*, vol. 162, 2022, pp. 23 965–23 998.
- [35] B. Neyshabur, H. Sedghi, and C. Zhang, "What is being transferred in transfer learning?" in *Advances in Neural Information Processing Systems*, 2020.
- [36] P. Izmailov, D. Podoprikin, T. Garipov, D. P. Vetrov, and A. G. Wilson, "Averaging weights leads to wider optima and better generalization," in *Conference on Uncertainty in Artificial Intelligence*, 2018.
- [37] Z. Li, W. Wang, J. Li, K. Chen, and S. Zhang, "Ucg: A universal cross-domain generator for transferable adversarial examples," *IEEE Transactions on Information Forensics and Security*, vol. 19, pp. 3023–3037, 2024.
- [38] B. Yang, H. Zhang, Y. Zhang, K. Xu, and J. dong Wang, "Adversarial example generation with adabelief optimizer and crop invariance," *Applied Intelligence*, vol. 53, pp. 2332–2347, 2021.
- [39] X. Wang, K. Tong, and K. He, "Rethinking the backward propagation for adversarial transferability," in *Advances in Neural Information Processing Systems*, 2023.
- [40] Z. Yuan, J. Zhang, and S. Shan, "Adaptive image transformations for transfer-based adversarial attack," in *European Conference on Computer Vision*, 2022.
- [41] J. Weng, Z. Luo, S. Li, N. Sebe, and Z. Zhong, "Logit margin matters: Improving transferable targeted adversarial attack by logit calibration," *IEEE Transactions on Information Forensics and Security*, 2023.
- [42] H. Chen, Y. Zhang, Y. Dong, and J. Zhu, "Rethinking model ensemble in transfer-based adversarial attacks," *ArXiv*, vol. abs/2303.09105, 2023.
- [43] X. Wang and K. He, "Enhancing the Transferability of Adversarial Attacks through Variance Tuning," in *CVPR*, 2021, pp. 1924–1933.
- [44] X. Wang, X. He, J. Wang, and K. He, "Admix: Enhancing the Transferability of Adversarial Attacks," in *Proceedings of the IEEE Conference on Computer Vision and Pattern Recognition (CVPR)*, 2021, pp. 16 158–16 167.
- [45] Y. Long, Q. Zhang, B. Zeng, L. Gao, X. Liu, J. Zhang, and J. Song, "Frequency Domain Model Augmentation for Adversarial Attack," in *European Conference on Computer Vision*, 2022, pp. 549–566.
- [46] A. Ganeshan, S. Vivek B., and R. V. Babu, "Fda: Feature disruptive attack," *2019 IEEE/CVF International Conference on Computer Vision (ICCV)*, pp. 8068–8078, 2019.
- [47] A. Kurakin, I. J. Goodfellow, and S. Bengio, "Adversarial Machine Learning at Scale," in *ICLR*, 2017.
- [48] F. Tramèr, A. Kurakin, N. Papernot, I. Goodfellow, D. Boneh, and P. McDaniel, "Ensemble Adversarial Training: Attacks and Defenses," in *ICLR*, 2018.
- [49] F. Liao, M. Liang, Y. Dong, T. Pang, X. Hu, and J. Zhu, "Defense against adversarial attacks using high-level representation guided denoiser," in *Proceedings of the IEEE Conference on Computer Vision and Pattern Recognition*, 2018, pp. 1778–1787.
- [50] C. Xie, J. Wang, Z. Zhang, Z. Ren, and A. Yuille, "Mitigating adversarial effects through randomization," in *Proceedings of International Conference on Learning Representations*, 2018.
- [51] J. M. Cohen, E. Rosenfeld, and J. Z. Kolter, "Certified Adversarial Robustness via Randomized Smoothing," *International Conference on Machine Learning*, pp. 1310–1320, 2019.
- [52] M. Naseer, S. Khan, M. Hayat, F. S. Khan, and F. Porikli, "A self-supervised approach for adversarial robustness," in *Proceedings of the IEEE/CVF Conference on Computer Vision and Pattern Recognition*, 2020, pp. 262–271.
- [53] W. Xu, D. Evans, and Y. Qi, "Feature squeezing: Detecting adversarial examples in deep neural networks," in *Proceedings of Network and Distributed System Security Symposium*, 2018.
- [54] A. Kurakin, I. J. Goodfellow, and S. Bengio, "Adversarial examples in the physical world," in *Artificial Intelligence Safety and Security*, 2018, pp. 99–112.
- [55] Z. Zhao, Z. Liu, and M. Larson, "Towards large yet imperceptible adversarial image perturbations with perceptual color distance," in *CVPR*, 2020.
- [56] O. Russakovsky, J. Deng, H. Su, J. Krause, S. Satheesh, S. Ma, Z. Huang, A. Karpathy, A. Khosla, M. Bernstein *et al.*, "Imagenet Large Scale Visual Recognition Challenge," *International Journal of Computer Vision*, vol. 115, pp. 211–252, 2015.
- [57] C. Szegedy, V. Vanhoucke, S. Ioffe, J. Shlens, and Z. Wojna, "Rethinking the inception architecture for computer vision," in *Proceedings of the IEEE Conference on Computer Vision and Pattern Recognition*, 2016, pp. 2818–2826.
- [58] C. Szegedy, S. Ioffe, V. Vanhoucke, and A. A. Alemi, "Inception-v4, inception-resnet and the impact of residual connections on learning," in *Thirty-first AAAI Conference on Artificial Intelligence*, 2017.
- [59] Z. Liu, Y. Lin, Y. Cao, H. Hu, Y. Wei, Z. Zhang, S. Lin, and B. Guo, "Swin transformer: Hierarchical vision transformer using shifted windows," in *Proceedings of the IEEE/CVF International Conference on Computer Vision*, 2021, pp. 10 012–10 022.
- [60] Z. Wang, A. C. Bovik, H. R. Sheikh, and E. P. Simoncelli, "Image quality assessment: from error visibility to structural similarity," *IEEE Transactions on Image Processing*, vol. 13, pp. 600–612, 2004.
- [61] R. Zhang, P. Isola, A. A. Efros, E. Shechtman, and O. Wang, "The unreasonable effectiveness of deep features as a perceptual metric," *2018 IEEE/CVF Conference on Computer Vision and Pattern Recognition*, pp. 586–595, 2018.
- [62] B. Zhou, A. Khosla, À. Lapedriza, A. Oliva, and A. Torralba, "Learning deep features for discriminative localization," *2016 IEEE Conference on Computer Vision and Pattern Recognition (CVPR)*, pp. 2921–2929, 2016.